Environmental Toxicology and Pharmacology 111 (2024) 104568

Contents lists available at ScienceDirect

Environmental Toxicology and Pharmacology

journal homepage: www.elsevier.com/locate/etap

Calcitriol/vitamin D receptor system alleviates PM2.5-induced human bronchial epithelial damage through upregulating mitochondrial bioenergetics in association with regulation of HIF-1α/PGC-1α signaling

Anyamanee Chatsirisupachai [a], Phetthinee Muanjumpon [b], Saowanee Jeayeng [c,d], Tasanee Onkoksong [b], Mutita Pluempreecha [b], Tanyapohn Soingam [b], Uraiwan Panich [b,*]

[a] Princess Srisavangavadhana College of Medicine, Chulabhorn Royal Academy, Bangkok 10210, Thailand
[b] Department of Pharmacology, Faculty of Medicine Siriraj Hospital, Mahidol University, Bangkok 10700, Thailand
[c] Department of Medical Science, School of Medicine, Walailak University, Nakhon Si Thammarat 80160, Thailand
[d] Research Center in Tropical Pathobiology, Walailak University, Nakhon Si Thammarat 80160, Thailand

ARTICLE INFO

"Edited by Dr. Malcolm D Tingle"

Keywords:
Calcitriol
Human bronchial epithelial cells
Hypoxia-inducible factor 1-alpha (HIF-1α)
Mitochondrial bioenergetics
Particulate matter ≤ 2.5 μm (PM 2.5)

ABSTRACT

PM2.5 exposure causes lung injury by triggering oxidative stress, mitochondrial dysfunction, and modulating HIF-1α signaling. Calcitriol activates VDR, which regulates cellular homeostasis. This study evaluated the protective role of the calcitriol/VDR system in PM2.5-induced damage to BEAS-2B bronchial epithelial cells by reducing oxidative stress, upregulating mitochondrial bioenergetics, and downregulating HIF-1α. We found that the calcitriol/VDR system decreased ROS formation and restored mitochondrial bioenergetics in PM2.5-treated cells. This improvement correlated with reduced HIF-1α nuclear translocation and increased PGC-1α protein and mitochondrial gene expressions. This study is the first to suggest that targeting the calcitriol/VDR system could be a promising pharmacological strategy for mitigating PM2.5-induced lung epithelial damage by promoting mitochondrial bioenergetics and regulating PGC-1α and HIF-1α signaling.

1. Introduction

Particulate matter (PM) is a key indicator of air pollution, one of the major environmental health risks worldwide (Kim et al., 2015). Long-term exposure to PM ≤ 2.5 μm (PM2.5) is associated with an increased risk of respiratory diseases including lung cancer as PM2.5 can penetrate deep into the lungs (Cao et al., 2018; Guo et al., 2020; Orakij et al., 2017; Pinichka et al., 2017; Pun et al., 2017; Wiwanitkit, 2016). The carcinogenic mechanisms of PM2.5 are linked to oxidative damage and signaling pathways involved in inflammation and apoptosis, which promote lung tumorigenesis (Ding et al., 2021; Li et al., 2020; Liu et al., 2018). In addition, oxygen is essential for metabolic homeostasis and energy production to maintain cellular function. The regulation of apoptosis, redox balance, and energy metabolism are profoundly influenced by mitochondria (Luo et al., 2020). Exposure to environmental toxicants, which induced reactive oxygen species (ROS) production, has been shown to cause mitochondrial dysfunction, a predominant pathological feature in respiratory diseases (Chakraborti et al., 2020; Dai et al., 2016). Hypoxia-inducible factor (HIF-1α) is a crucial transcription factor mediating adaptive responses to oxidative stress and plays a vital role in the crosstalk between inflammation and oxidative stress in hypoxia, contributing to lung carcinogenesis (Li et al., 2019; McGarry et al., 2018). Peroxisome proliferator-activated receptor coactivator (PGC-1α) is a transcriptional coactivator characterized as a master regulator of mitochondrial biogenesis (O'Hagan et al., 2009).

Vitamin D deficiency is well known for its association with an

Abbreviations: ATP5F1B, ATP Synthase F1 Subunit Beta, gene encodes a subunit of mitochondrial ATP synthase gene; BEAS-2B, normal human bronchial epithelial cell line; BNIP3, BCL2 interacting protein 3; *CYCS*, cytochrome C, Somatic gene; HIF-1α, hypoxia-inducible factor 1-alpha; LDHA, lactate dehydrogenase A; *SOD2*, superoxide dismutase 2, also known as manganese superoxide dismutase MnSOD, gene encodes manganese superoxide dismutase enzyme located in the mitochondrial matrix gene; PDK1, pyruvate dehydrogenase kinase 1; PGC-1α, peroxisome proliferator-activated receptor gamma co-activator 1 alpha; PM 2.5, particulate matter ≤ 2.5 μm; *SIRT3*, sirtuin 3, gene encodes mitochondria-localized tumor suppressor gene; ROS, reactive oxygen species; VDR, vitamin D receptor.

* Correspondence to: Department of Pharmacology, Faculty of Medicine Siriraj Hospital, Mahidol University, 2 Wanglang Rd., Bangkok Noi, Bangkok 10700, Thailand.

E-mail address: uraiwan.pan@mahidol.ac.th (U. Panich).

https://doi.org/10.1016/j.etap.2024.104568
Received 9 April 2024; Received in revised form 7 September 2024; Accepted 19 September 2024
Available online 21 September 2024

increased risk of skeletal diseases and fractures. Poor dietary intake of vitamin D has also been reported to affect respiratory health and is associated with an increased risk of pulmonary diseases including lung cancer and asthma (Tretli et al., 2012). Provitamin D3 (7-dehydrocholesterol) is converted to pre-calciferol, an intermediate in the production of and cholecalciferol, although these elements are inactive forms of vitamin D (Bikle, 2014). Calcitriol, an active metabolite of vitamin D containing three hydroxyl (OH) groups, is commonly referred to as 1,25-dihydroxycholecalciferol, or 1,25-dihydroxyvitamin D_3 (1,25 $(OH)_2D_3$) (Bhattarai et al., 2020; Tanakol et al., 2018). The binding of calcitriol to the vitamin D receptor (VDR) allows VDR to form a heterodimer with the retinoid x receptor (RXR). This VDR-RXR heterodimer then binds to vitamin D-responsive elements (VDRE) promoter to mediate the transcription of genes involved in regulating antioxidant defense system, inflammatory response and cellular functions including cell proliferation, cell differentiation and apoptosis (Dominguez et al., 2021; Kim et al., 2020; Quesada-Gomez et al., 2020; Zhang et al., 2017). Previous reports have demonstrated that calcitriol administration exerts beneficial effects against acute lung injury due to its immunomodulatory and anti-inflammatory properties (Tan et al., 2016; Yeh et al., 2022, 2021). However, the protective role of calcitriol in PM2.5-induced lung epithelial damage via the promotion of mitochondrial function in association with the regulation of HIF-1α translocation activity has not been explored. In this study, we assessed the mechanisms underlying the protective effects of the calcitriol/VDR axis against PM2.5-induced human bronchial epithelial damage by evaluating oxidative stress, mitochondrial bioenergetics and related genes as well as HIF-1α translocation activity using a cultured BEAS-2B human bronchial epithelial cell model. As shown in the graphical abstract, understanding the pharmacological role of the calcitriol/VDR system could give insights into a promising novel approach for preventing lung damage from air toxicants.

2. Materials and methods

2.1. Cell culture and treatment approach

Human non-tumorigenic lung epithelial cell line, the BEAS-2B cell line was derived from human bronchial tissue and has since been widely utilized as an *in vitro* non-tumorigenic lung epithelial model for lung dysfunction as well as carcinogenesis. BEAS-2B cells were grown on the plates in the presence of the Dulbecco's Modified Eagle Medium (DMEM; Invitrogen life Technologies, France) supplemented with 10 % Fetal Bovine Serum (FBS) (Millipore, USA). The cells were grown to 90 % confluence and passaged by trypsin/EDTA. Briefly, cells were seeded in 6-well and 96-well culture plates and treated with test compounds at ~80 % confluence.

2.2. Treatment model: PM2.5 treatment

In this study, urban fine particulate matter (<4 μm) (SRM2786) was obtained from the National Institute of Standards and Technology (NIST). The reagent was produced under the standard procedure which existing the air particulate matter with appropriate certified reference material (CRM) from NIST. The purpose of the Standard Reference Material (SRM) 2786 is to assess analytical techniques for the identification of PM2.5 particles which contain (PAHs), nitro-substituted PAHs (nitro-PAHs), polybrominated diphenyl ether (PBDE) congeners, hexabromocyclododecane (HBCD) isomers, sugars, polychlorinated dibenzo-p-dioxin (PCDD) and dibenzofuran (PCDF) congeners, inorganic constituents, and other particle-size characteristics in atmospheric particulate material. All the following constituents provided are naturally present in the particulate matter. PM2.5 at doses of 25–400 μg/mL have been employed to study its cytotoxic effect on A549 cell, the human respiratory cells (Veerappan et al., 2019). In addition, the PM2.5 doses at 10–100 μg/mL and the exposure time up to 24 h were generally obtained to investigate the harmful effects of air pollutant toxicology including the oxidative stress and the inflammation in the cell culture (Huang et al., 2018; Jin et al., 2018; Yang et al., 2019). In this study, PM2.5 at doses of 25, 50, 100, and 200 μg/mL were employed to determine a dose-dependent stimulation of ROS formation.

2.3. Treatment model: calcitriol treatment

Calcitriol, a synthetic (man-made) active form of vitamin D_3 (cholecalciferol) and known as 1,25-dihydroxycholecalciferol, activates the vitamin D receptor in the nucleus to produce the downstream signaling genes. The calcitriol at doses of 0.5–100 nM was previously used to study its cytoprotective role via modulating the mitochondria channels (Gesmundo et al., 2020; Gonzalez et al., 2019; Olszewska et al., 2022). In this study, we thus used calcitriol at dose 1, 10, and 100 nM for assessing its role in regulating the cellular adaptive response to PM2.5 and mitochondrial functions.

BEAS-2B cells were pre-treated individually with ethanol (sham control group, 1:1000 dilution) or calcitriol (1, 10, 100 nM) prior to treatment with the PM2.5 solution (the product label: SRM 2786, NIST, USA) for various time-point upon the experimental detection. After PM2.5 incubation, cells were harvested at 1, 3, 5, 6, and 24 h for further detections of cell viability, ROS formation, oxygen consumption rate, mRNA and protein expressions, respectively. A substantial increase in ROS formation was observed in BEAS-2B cells treated with PM2.5 at dose of 100 μg/mL and 100 μg/mL of PM2.5 was thus selected to induce BEAS-2B cell injury in further experiments.

2.4. Cell survival determination using MTT assay

BEAS-2B cells treated with PM2.5 at three different doses (50, 100, and 200 μg/mL) were obtained to test the cell viability prior to conducting further experiments. Cells were cultured in 96-well plates at a density of 5×10^3 cells per well. Following the appropriate treatment, 10 μL of MTT solution was added to each well, allowed to incubate for 2 h. After the supernatant was discarded, the 120 μL DMSO was added, and the absorbance was then read at 490 nm with a microplate analyzer.

2.5. Determination of intracellular reactive oxygen species (ROS) formation using flow cytometry

The treated cells were incubated for 30 min at 37°C in PBS containing 5 μM non-fluorescent dichlorofluorescein (H_2DCFDA). The detection of ROS levels is based on intracellular ROS oxidizing H_2DCFDA to create fluorescent 2,7-DCF. H_2DCFDA, which permeates cells and accumulates mostly in the cytoplasm. Intracellular esterases deacetylated the penetrated H_2DCFDA to provide a non-fluorescent product (H_2DCF). By utilizing a fluorescence activated cell sorter (FACS-calibur), as previously described, the fluorescence reflected the oxidized form in cells were visualized and detected by flow cytometry (Lohakul et al., 2022).

2.6. Assessment of mitochondrial function by Seahorse XFp analyzer

The measurement of the Seahorse XFp Extracellular Flux Analyzer (Agilent Technologies, Bucher Biotec, Basel, Switzerland) was used to measure mitochondrial respiration in a real time. One day prior to analysis, cells were seeded overnight on Seahorse XFp Fluxpak. Oxygen consumption rate (OCR) was detected by a consecutive injection of modulators. Oligomycin (5 mM), the first modulator, was employed to access ATP production rate and proton (H+) leak and, following OCR measurement, carbonyl cyanide-4-(trifluoromethoxy) phenylhydrazone (FCCP; 2 μM), the second modulator, was used to estimate the maximal respiration and the spare (or reserve) respiratory capacity. Antimycin A plus rotenone cocktail (0.5 μM), the third modulator, were employed together to detect residual of non-mitochondrial respiration rate. The

basal respiration was calculated by subtracting the non-mitochondrial respiration from the basal OCR prior to the oligomycin injection. Coupling efficiency (%) was the percentage calculated from the ATP production rate divided by the basal respiration rate. The oxygen levels in each time-point detection represented the capability of protein complex for utilize the oxygen in each mitochondrial complex, complex I-IV. Seven assay parameters were analyzed as following: basal respiration (pMoles/min), ATP production (pMoles/min), proton leak (pMoles/min), maximal respiratory (pMoles/min), spare respiratory capacity (pMoles/min), coupling efficiency (%), and non-mitochondrial respiration (%) as previously described (Lohakul et al., 2022). The OCR data was normalized using the Bradford assay detecting protein concentration of each treated cells and was presented as pMoles/min/*mg* protein in the graph analysis.

2.7. Heat map analysis of mRNA expression using the quantification of Real-time RT-PCR

Cells were incubated with 100 μg/mL PM2.5 solution for 1, 3, 6, and 24 h for mRNA detection. Cell pellets were obtained to isolate the RNA using the illustra RNAspin Mini RNA Isolation Kit (GE Healthcare, UK). Reverse transcription was carried out with an equal amount of 1 *mg* RNA using the Improm-II reverse transcriptase (Promega, Medison, USA). Real-time RT-PCR reactions were performed in triplicate for each sample. The ABI Prism 7500 Real Time PCR System (Applied Biosystems, USA) was obtained for the measurement of amplification under the following amplification conditions: 95 °C for 10 min; 40 cycles of 95 °C for 15 s; 60 °C for 40 s; and 72 °C for 40 s. The reactions were performed in a total volume of 10 µl of reaction mixtures containing the cDNA template plus FastStart universal SYBR Green Master (ROX) and 10 µM concentrations of primers as previous described (Chaiprasongsuk et al., 2020, 2017). PCR primer sequences were designed using the Primer Express software version 3.0 (Applied Biosystems, USA). The forward and reverse primer sequences were shown in the supplemental table1. The mean of fold-change of each gene was normalized with the housekeeping gene, GAPDH mRNA using the ΔΔCt method. The modulation in gene expressions are presented as the average of fold-change with statistically significant differences indicated. The statistical student t-test was used for the comparison with non-treatment or PM2.5 treated cells, The P value is reported as * $P < 0.05$, ** $P < 0.01$, and *** $P < 0.001$ for the sham-control cells versus PM2.5-treated cells, while the $\#P<0.05$, $\#\#P< 0.01$, $\#\#\#P< 0.001$ was compared between calcitriol treatment versus cells pretreated with PM2.5 alone. Heat map of each gene was graded and generated using Prism (GraphPad Software Inc.).

2.8. Immunofluorescent analysis of VDR and HIF-1α protein expression

Cells plated in 96-well plate were obtained for the immunofluorescent assay. After the treatment, cells were further fixed in 4 % paraformaldehyde (PFA) for 10 min at room temperature and washed three times with 0.1 % Triton X-100 (BioRad, Hercules, CA) in PBS to permeabilize membrane. Blocking solution (1 % BSA in PBS) was added into each well for 1 h at room temperature. Cells were then incubated with anti-HIF-1 alpha mouse monoclonal antibody (H1alpha67) (ab1; abcam) and anti-VDR mouse monoclonal antibody (D-6) (sc-13133; santa cruz) at the dilution of 1:100 in blocking solution overnight at 4°C. Anti-mouse IgG H&L (Alexa Fluor® 488) solution (ab150113; abcam) was then incubated for 1 h. After washing with PBS, nuclei were stained with DAPI dye. Stained cells were imaged at 40X magnification imaged and analyzed with Operetta CLS High-Content Analysis System (PerkinElmer Inc., USA). The analysis of fluorescent intensity was performed by the calculation of the fluorescent-nuclear/cytosolic protein ratio and shown in histograms as the mean of the fold change ± SD using the Columbus Image Data Storage and Analysis System (PerkinElmer Inc., USA). Data was normalized using the protein concentration of each treated cells performed by the Bradford assay as previous described (Lohakul et al., 2022).

2.9. PGC-1α protein expression analysis by western blotting

Cells were incubated with 100 μg/mL PM2.5 solution for 12 h for PGC-1α protein detection. Cell pellets were obtained to isolate the whole cell extraction using the NP-40 lysis buffer. Lysed cells were then quantified protein concentration by the Bradford assay prior to performing the SDS-PAGE electrophoresis and blotting. The primary antibody of PGC-1α, Anti-PGC-1α mouse monoclonal antibody (D-5) (sc-518025; santa cruz) was added to detect the immunoblotting. The secondary antibody, anti- mouse tagged with the horseradish peroxidase (HRP) was the performed the fluorescent prob detection on the GelDoc Imaging System (Bio-Rad). The band intensities from immunoblotting were quantified using Image Lab version 6.1 software (Bio-Rad). Protein expression was normalized and presented as a percentage of the control cells (untreated cells) ± SD.

2.10. Statistical analysis

Data are expressed as the mean ± standard deviation of at least three independent experiments ($n \geq 3$) performed on different days using freshly prepared reagents. PM2.5-treated and control groups were analyzed by Student's t-test; *$p < 0.05$, **$p < 0.01$, ***$p < 0.001$. A one-way analysis of variance (ANOVA) followed by Dunnett's Test was used to analyze the differences between the PM2.5-treated group and the PM2.5-treated with compound treatment groups; #$p < 0.05$, ##$p < 0.01$, ###$p < 0.001$, considered statistically significant. All analyses were performed using Prism (GraphPad Software Inc.).

3. Results

3.1. Calcitriol/VDR system protected against the ROS formation in BEAS-2B human bronchial epithelial cells exposed to PM2.5

Previous studies reported that less than 50 % cytotoxicity was observed in BEAS-2B treated with PM2.5 at doses between 6.25 and 200 μg/mL (Jiang et al., 2021; Niu et al., 2020; Wu et al., 2017). Consequently, this study aimed to test the effects of PM2.5 at doses ranging from 50 to 200 μg/mL on BEAS-2B cell viability to confirm the non-cytotoxic effects of PM2.5. As shown in supplemental Fig. 1, PM2.5 at doses of 50–200 μg/mL had no significant effect on cell survival, ensuring that the observed effects on oxidative stress and mitochondrial function were due to specific cellular stress responses to PM2.5 exposure, supporting further studies with PM2.5 at these doses.

Exposure to PM2.5 can induce lung injury via ROS formation, leading to oxidative damage in airway epithelial cells (Lelieveld et al., 2021; Mazuryk et al., 2020). Hence, we studied the protective effects of calcitriol on PM2.5-induced oxidative stress in lung epithelium. First, we investigated the dose- and time-dependent effects of PM2.5-induced ROS formation in BEAS-2B cells. An early stimulation (1-h incubation) of oxidative stress by PM2.5 was found at doses of 25, 50, and 100 μg/mL. Following 6-h incubation, oxidative stress was induced by treatment with PM2.5 at doses of 100 and 200 μg/mL. PM2.5 at 100 μg/mL caused a significant increase in ROS formation at both 1 h and 6 h post-PM2.5 exposure (Fig. 1A). We then investigated the protective effect of calcitriol on ROS formation induced by PM2.5 at 100 μg/mL and observed that pre-treatment with calcitriol at 1, 10, and 100 nM significantly reduced ROS levels at 1 h post-PM2.5 exposure compared to the PM2.5-treated cells without calcitriol (Fig. 1B). The sham treatment (ethanol solution at 1:1000 dilution) did not affect ROS levels as the sham group exhibited similar ROS levels to the control (non-treatment) group (Fig. 1C).

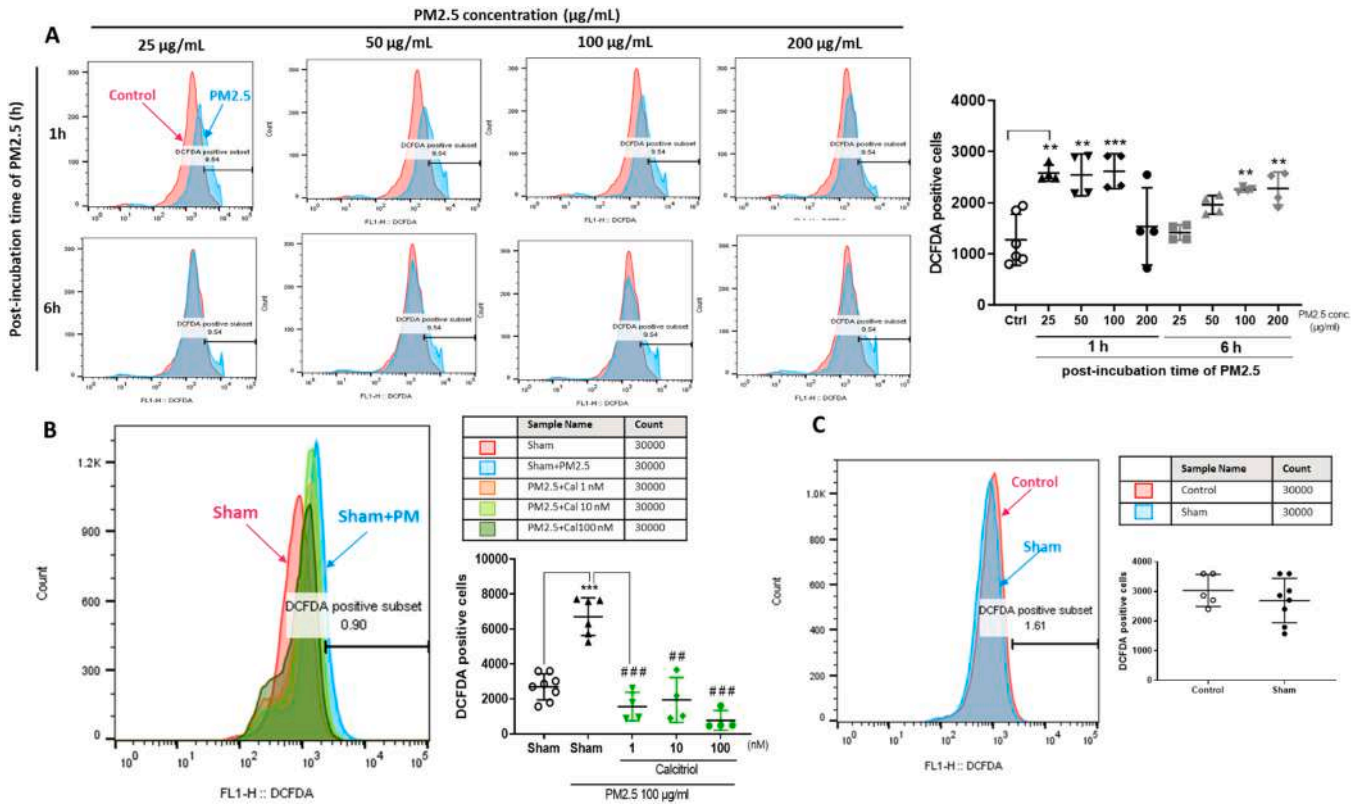

Fig. 1. Calcitriol protected against the induction of ROS formation in BEAS-2B cells exposed to PM2.5. To investigate the protective effects of calcitriol against PM2.5-induced ROS formation in BEAS-2B cells, exposure to PM2.5 at doses of 25, 50, 100, and 200 μg/mL for 1 and 6 h was performed to evaluate the dose- and time-dependent effects. (A) The histogram of flow cytometry shows cells stained with DCFDA fluorescent dye, and the bar graph represents the number of DCFDA-positive cells in PM2.5-exposed cells: control (pink histogram) versus cells treated with PM2.5 at 25–200 μg/mL. (B) The histogram of flow cytometry and the bar graph represent the number of DCFDA-positive cells in calcitriol-treated cells following 1 h of PM2.5 incubation, indicated as PM2.5+Cal groups. (C) ROS formation in BEASE-2B cells under sham treatment (ethanol vehicle solution; 1:1000 dilution) compared to non-treatment (control or ctrl group; serum-free medium without ethanol solution). The histogram of flow cytometry showed cells stained with DCFDA fluorescent dye, while the bar graph represents the number of DCFDA positive cells in ethanol treatment (sham group; black bar) compared to non-treatment (control group; white bar). Statistical analysis between the non-treated PM2.5 control and PM2.5-treated cells was conducted using Student's *t* test, and the comparison between PM2.5-pretreated cells with (green dot plot graph) and without (black dot plot graph) calcitriol treatment was performed using one-way ANOVA with Dunnett's multiple comparison test. **P< 0.01, ***P< 0.001versus sham-control cells without PM2.5 and ##P< 0.01, ###P< 0.001 versus PM2.5-treated cells without calcitriol, n ≥ 3.

3.2. Calcitriol/VDR system restores mitochondrial bioenergetics in PM2.5-exposed lung epithelial cells

Oxygen utilization in the mitochondria is a key component of cellular metabolic processes including cellular respiration and energy production. Several mitochondrial components, such as protein complex I-IV and the ATP synthase complex, are crucial for these processes (Mori et al., 2021; Needs et al., 2021). Excess ROS can disrupt the mitochondrial respiratory chain, a vital part of energy metabolism. PM2.5 contains chemical constituents such as sulfate, nitrate, ammonium, elemental carbon, organic carbon, silicon, and sodium ion, which possess carcinogenic, allergenic, and toxic properties (Dominici et al., 2015; Toro-Heredia et al., 2021). Exposure of BEAS-2B cells to PM2.5 (50, 100, and 200 μg/mL) caused a significant reduction in mitochondrial function, as indicated by impaired oxygen consumption rate (OCR) of cells (Fig. 2A) and mitochondrial respiratory functions (Fig. 2B-H). We then tested the protective effects of calcitriol against PM2.5 (200 μg/mL)-induced compromised mitochondrial respiration. Fig. 3A shows the kinetics of bioenergetics measured by OCR, presented as the pMoles/min/*mg* protein, for 0–80 min. As shown in Fig. 3A, OCR decreased in the PM2.5-treated sham group compared to the sham-control group, suggesting reduced oxygen utilization in response to PM2.5 exposure. In contrast, treatment with calcitriol at 1, 10, and 100 nM led to a recovery of PM2.5-induced OCR reduction. We also investigated mitochondrial respiration parameters, as shown in Fig. 3. Fig. 3A represents an overview of cellular kinetic changes in OCR over 80 min, with each mitochondrial function parameter elaborated in Fig. 3B-H. PM2.5 exposure significantly impaired multiple mitochondrial bioenergetic parameters, including maximal respiratory capacity (Fig. 3B), non-mitochondrial respiration (Fig. 3C), basal respiration (Fig. 3D), proton leak (Fig. 3E), ATP production (Fig. 3F), spare respiratory capacity (%) (Fig. 3G) in the PM2.5-treated sham group compared to the sham-control group, * $p < 0.05$, **$p < 0.01$, ***$p <$ 0.001 versus sham-control cells. However, treatment with calcitriol at certain concentrations restored mitochondrial respiration, with significant increases in maximal respiration, proton leak, and spare respiration capacity, # $p < 0.05$, ## $p < 0.01$, ###$p < 0.001$ versus PM2.5-treated cells. Sham treatment (ethanol solution at 1:1000 dilution) did not alter mitochondrial function compared to control (non-treatment) cells (Fig. 3A-H).

3.3. Calcitriol upregulated PGC-1α protein and its down-stream mitochondrial target genes in PM2.5-exposed lung epithelial cells

The transcriptional coactivator PGC-1 plays a key role in nuclear-mitochondrial gene transcription of respiratory complex proteins and promotes antioxidant and mitochondrial functions (Lin et al., 2002; Shan et al., 2022). Moreover, HIF-1α has been implicated in mitochondrial dysfunction through its co-regulation with the PGC-1 transcription coactivator (O'Hagan et al., 2009). We evaluated the role of the

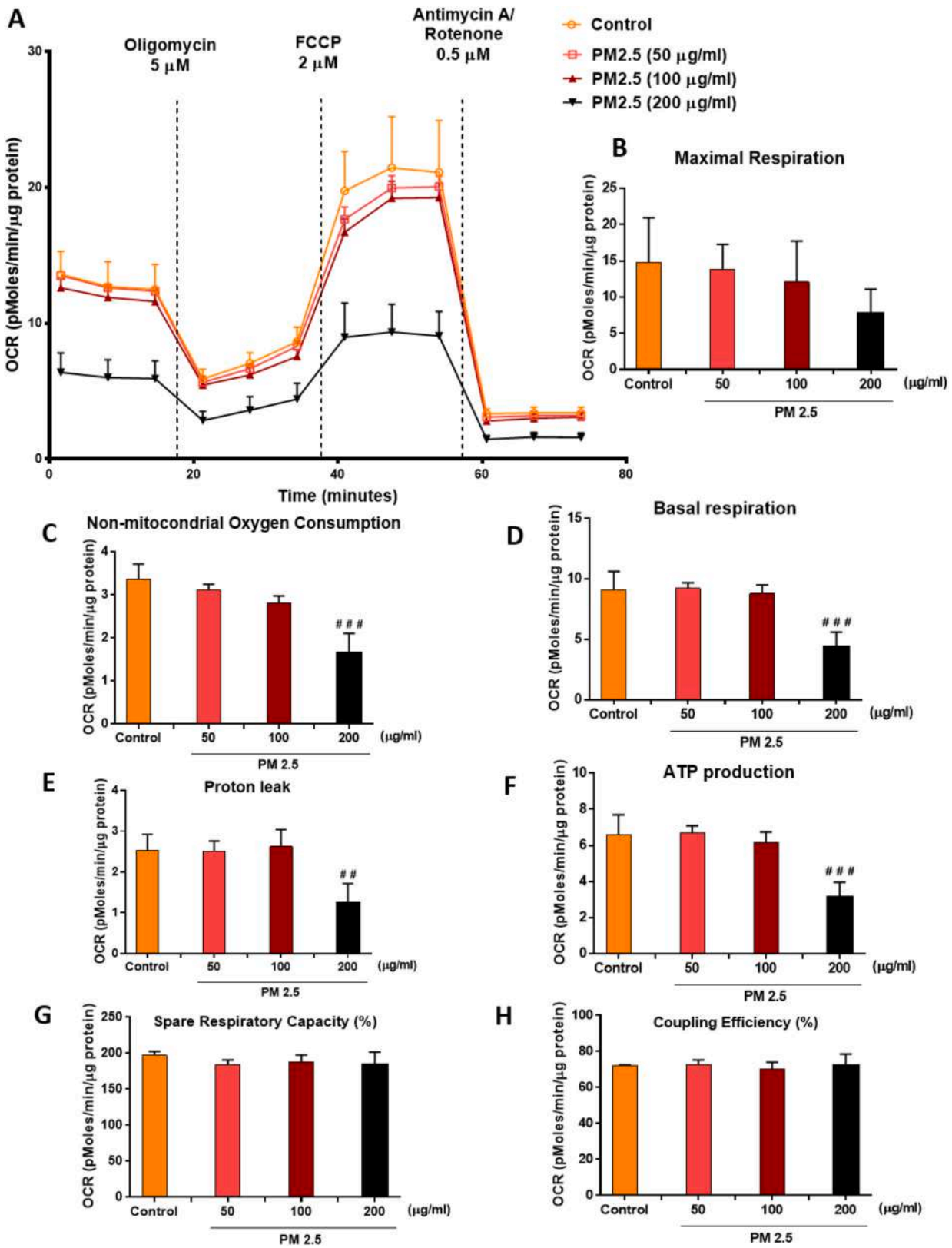

Fig. 2. The dose-dependent effects of PM2.5 treatment on oxygen consumption rate and mitochondrial functions**.** (A) The oxygen consumption rate (OCR) measured at repeated 6-minute intervals, along with mitochondrial assay parameters including (B) maximal respiratory capacity, (C) non-mitochondrial respiration, (D) basal respiration, (E) proton leak, (F) ATP production, (G) spare respiratory capacity (%), and (H) coupling efficiency (%). Data were normalized to protein concentration (mg) and presented as the pMoles/min/mg protein in the bar graph. Statistical analysis between PM2.5-treated cells (50, 100, and 200 μg/mL) and ethanol-treated cells (sham control cells, orange bar) was conducted using one-way ANOVA with Dunnett's multiple comparison test. #P<0.05, ##P< 0.01, ###P< 0.001versus non-treated with ethanol-treated cells, n $\geq$ 3.

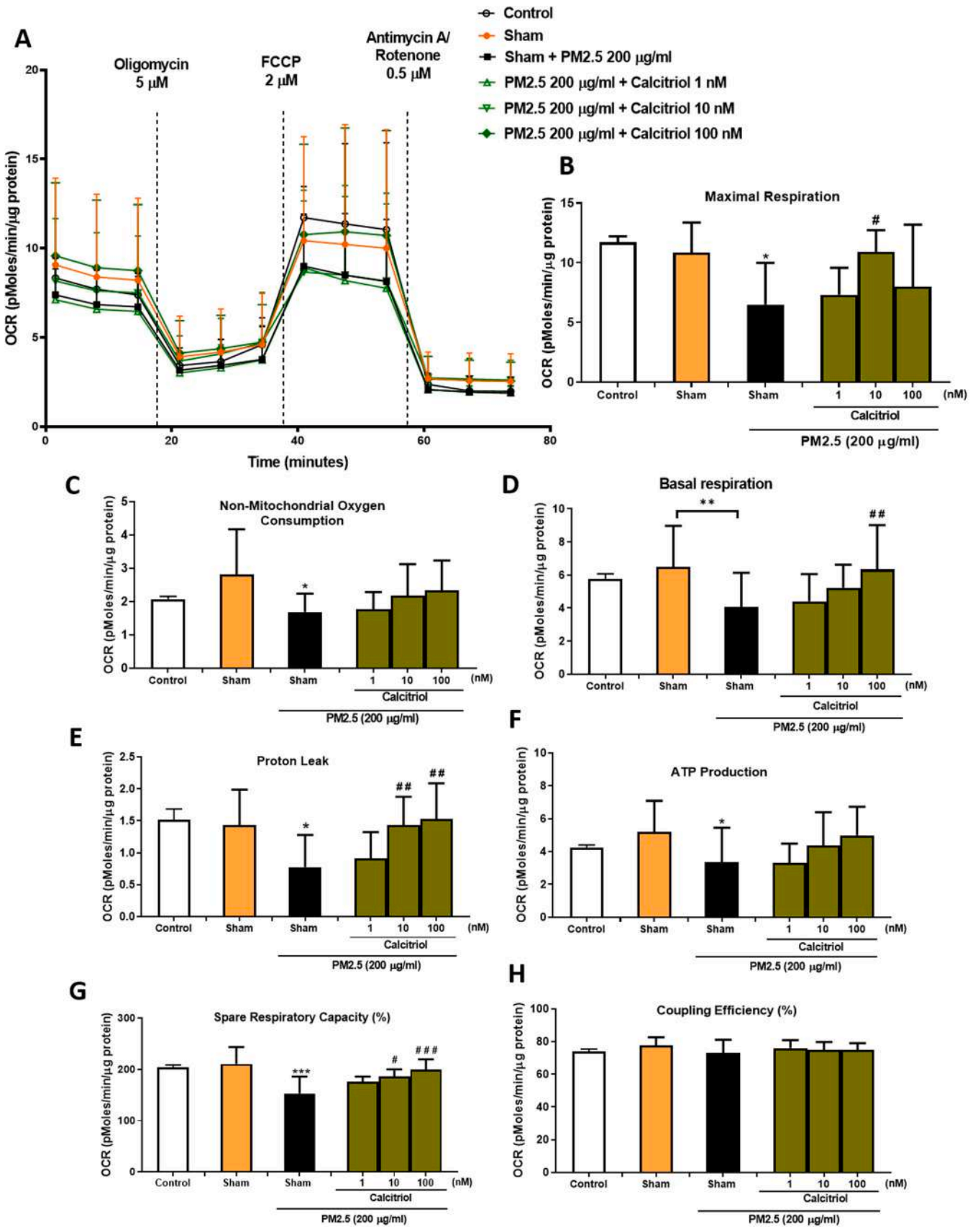

(caption on next page)

Fig. 3. Calcitriol restored oxygen consumption rate and mitochondrial function in PM2.5 exposed BEAS-2B cells. To evaluate the effects of calcitriol on the PM2.5-induced mitochondrial dysfunction in lung epithelial cells, we determined the oxygen consumption rate associated with mitochondrial function for each protein complex. BEAS-2B cells were treated with ethanol vehicle solution (1:1000 dilution; sham group) or 1, 10, 100 nM for 16 h prior to incubation with 200 μg/mL PM2.5 for 5 h. (A) The oxygen consumption rate (OCR) measured at repeated 6-min intervals, along with mitochondrial assay parameters including (B) maximal respiratory capacity, (C) non-mitochondrial respiration, (D) basal respiration, (E) proton leak, (F) ATP production, (G) spare respiratory capacity (%), and (H) coupling efficiency (%). Data were normalized to protein concentration (mg) and presented as the pMoles/min/mg protein in the bar graph. The statistical analysis between the non-treated with PM2.5 control (orange bar graph) and PM2.5-treated cells (black bar graph) was performed using Student's *t* test, and between PM2.5-pretreated cells with (green bar graph) and without (black bar graph) calcitriol treatment using one-way ANOVA with Dunnett's multiple comparison test. *P<0.05, **P< 0.01, ***P< 0.001versus sham-control cells without PM2.5 and #P<0.05, ##P< 0.01, ###P< 0.001 versus PM2.5-treated cells without calcitriol, n ≥ 3.

calcitriol/VDR system in regulating PGC-1α and its downstream mitochondrial genes involved in OXPHOS subunits, mitochondrial DNA integrity, mitochondrial homoeostasis, metabolism of essential substrates and cofactors for cellular respiration and xenobiotic metabolism (Stenton and Prokisch, 2020). While a reduction in PGC-1α protein expression was observed in the PM2.5-treated cells compared to untreated cells, calcitriol treatment significantly increased PGC-1α protein expression compared to PM2.5-treated cells, suggesting the restoration of PGC-1α expression in PM2.5-exposed cells (Fig. 4A). Additionally, we assessed the effect of calcitriol on mitochondrial genes including ATP Synthase F1 Subunit Beta (*ATP5F1B*), cytochrome C, somatic (*CYCS*), Mn superoxide dismutase (*MnSOD* or *SOD2*) and sirtuin 3 (*SIRT3*), which reflect mitochondrial functions in PM2.5-treated cells (Boland et al., 2013; Calahorra et al., 2018). Alterations in mitochondrial gene expression were detected at various time points (1, 3, 6, and 24 h) following PM2.5 treatment. A significant downregulation of all four genes (*ATP5F1B*, *CYCS*, *MnSOD* and *SIRT3*) was observed at 24 h post-treatment in lung epithelial cells compared to non-treated control cells, *p < 0.05 versus non-treated control cells (Fig. 4B). Heatmap analysis was performed to represent differential gene expression between different treatment groups. The mean fold-change in mRNA expression was defined as upregulated expression (red) and downregulated (blue). Treatment of PM2.5-treated cells with calcitriol significantly induced mitochondrial-related genes compared to PM2.5-treated cells without calcitriol, as shown on the heatmap (Fig. 4C), # p< 0.05 versus PM2.5-treated cells, suggesting the protective role of calcitriol against PM2.5-induced downregulation of PGC-1α and its downstream mitochondrial genes. Mitochondrial-related genes were not significantly changed in the sham treatment (ethanol solution at 1:1000 dilution) compared to control (non-treatment) cells (Fig. 4C).

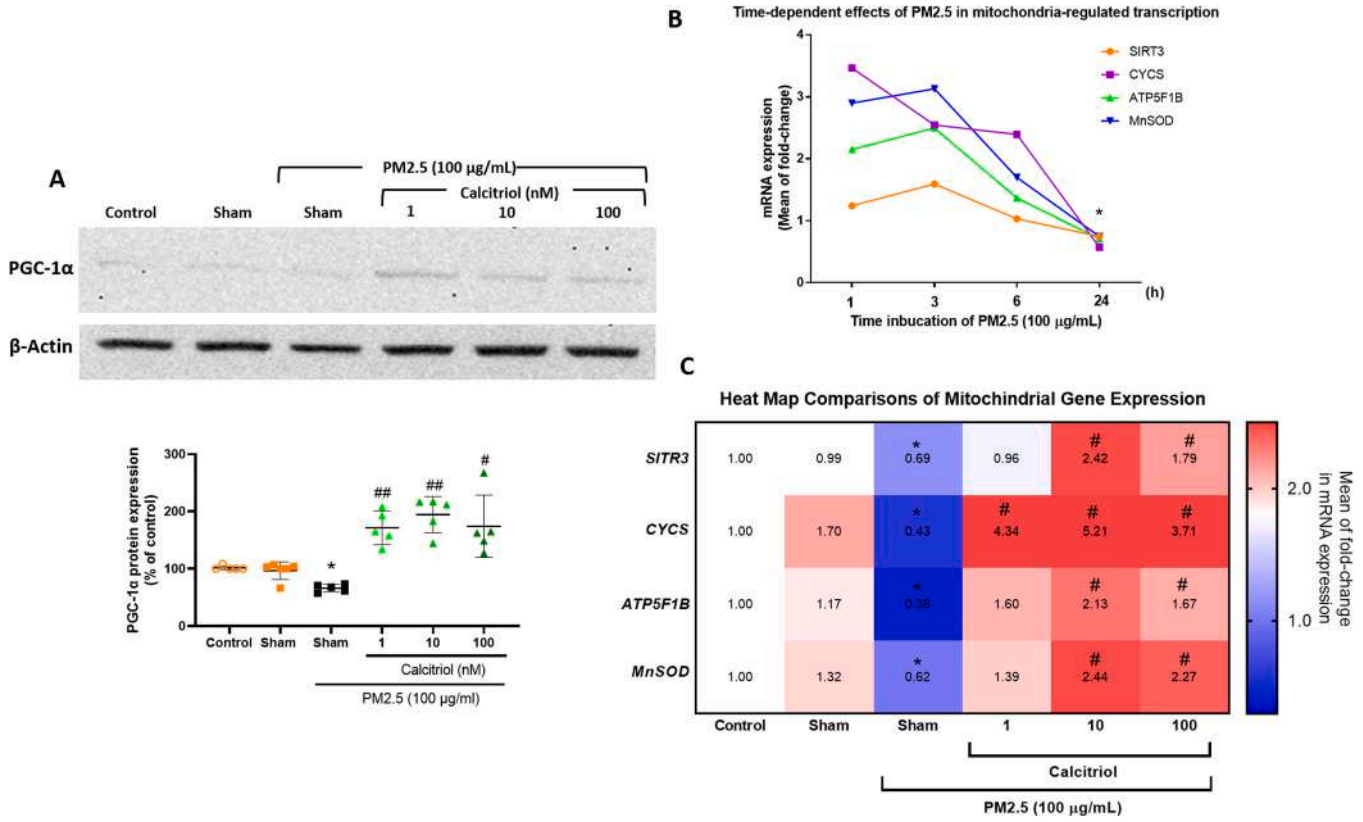

Fig. 4. The mechanistic role of vitamin D receptor activation on PGC-1α/mitochondrial bioenergetics and heat map analysis showing the regulation of mitochondrial-targeted genes. (A) Protein expression of PGC-1α in BEAS-2B cells treated with calcitriol, an activator of vitamin D receptor, prior to exposed with PM2.5 at dose 100 μg/mL. The mRNA expression levles of sirtuin 3 (*SITR3)*, cytochrome C, somatic (*CYCS*), ATP Synthase F1 Subunit Beta (*ATP5F1B*), Mn superoxide dismutase (*MnSOD* or *SOD2*) were analyzed to determine transcriptional functions in mitochondria. Each mRNA level of the targeted gene was normalized relative to the GAPDH mRNA levels and presented as the mean fold-change. (B) Time-dependent effects of PM2.5 on the mitochondrial target genes: *SITR3, CYCS, ATP5F1B, SOD2.* BEAS-2B cells were exposed with PM2.5 for 1, 3, 6, and 24 h. (C) Treatment groups compared to the ethanol sham group with or without PM2.5 exposure. Each horizontal row represents the same gene product, while each vertical row represents each sample. The fluorescence ranges from high (red) to low (blue), as indicated by the colored bar, reflecting the degree of gene expression. Statistical analysis between sham-control cells and PM2.5-treated cells was performed using Student's *t* test, and between PM2.5-pretreated cells with calcitriol and the cells treated with PM2.5 alone using one-way ANOVA with Dunnett's multiple comparison test. *P<0.05 versus non-treated with PM2.5 control cells, and #P<0.05 and ##P< 0.01 versus PM2.5-treated cells, n ≥3.

3.4. Calcitriol restored the nuclear translocation of VDR in PM2.5-exposed lung epithelial cells

The regulation of VDR plays a crucial role in promoting mitochondria function and protecting against oxidative stress-mediated respiratory cell damage (Ashcroft et al., 2020; Ricca et al., 2018). Upon binding with calcitriol, VDR forms a heterodimer with certain receptors, facilitating attachment to vitamin D response elements (VDRE) in the promoter region, thereby regulating the transcription of genes involved in cellular responses (Annamalai et al., 2021). We further investigated the role of calcitriol/VDR axis in protecting against PM2.5-mediated oxidative damage in BEAS-2B cells. Our time-dependent study on the effects of PM2.5 on the nuclear translocation of VDR (Fig. 5B) revealed that PM2.5 treatment significantly reduced the nuclear/cytosolic VDR protein ratio at 24 h post-treatment. Exposure to PM2.5 at 100 μg/mL significantly decreased VDR translocation in BEAS-2B lung cells (Fig. 5C, *$p< 0.01$ versus non-treated control cells). We then investigated the effects of calcitriol on PM2.5 (100 μg/mL)-induced downregulation of VDR nuclear translocation and mRNA levels (Fig. 5C, A). Image-based analysis showed that calcitriol treatment significantly induced VDR nuclear translocation and mRNA expressions compared to PM2.5-treated cells without calcitriol (Fig. 5C, A), #$p< 0.05$, ##$p< 0.01$, ###$p< 0.001$ versus PM2.5-treated cells. Additionally, calcitriol treatment alone significantly increased VDR mRNA expressions compared to the sham-control group (indicated by pink dot in Fig. 5A, *$p <0.05$ versus sham-control cells), supporting the effects of calcitriol on VDR nuclear translocation. Furthermore, neither VDR nuclear translocation nor mRNA expression levels were significantly changed in the sham treatment (ethanol solution at 1:1000 dilution) compared to control (non-treated) cells (Fig. 5C, A).

3.5. Calcitriol mitigated the nuclear translocation of HIF-1α and its downstream genes in PM2.5-exposed lung epithelial cells

HIF-1α, a dimeric protein complex, is a central physiological regulator of homeostatic process in response to oxygen insufficiency and is primary responsible for regulating cellular responses (Gaspar and Velloso, 2018; Kierans and Taylor, 2021). To understand the involvement of HIF-1α nuclear translocation in PM2.5-mediated cellular oxidative stress, we conducted an immunofluorescent study on the time-dependent effects of PM2.5. We observed an early increase in HIF-1α nuclear translocation in BEAS-2B cells (Fig. 6B) as exposure to PM2.5 at 100 μg/mL for 3 h caused a significant induction of the nuclear/cytosolic HIF-1α protein ratio compared to sham-control cells (*$p <0.05$ versus sham-control cells without PM2.5). We then assessed the effects of calcitriol on PM2.5-induced HIF-1α nuclear translocation and mRNA levels. Calcitriol treatment significantly reduced HIF-1α nuclear translocation and mRNA expression compared to PM2.5-treated cells without calcitriol (Fig. 6C, A), #$p< 0.05$, ##$p < 0.01$, ###$p < 0.001$ versus PM2.5-treated cells. Additionally, we investigated the mRNA expressions of HIF-1α target genes to confirm the effects of calcitriol on PM2.5-induced HIF-1α nuclear translocation. Cells pretreated with calcitriol for 16 h were exposed to PM2.5 at 100 μg/mL for 12 h and harvested to measure mRNA expressions of the HIF-1α target genes including *LDHA, BNIP3,* and *PDK1*. The induction of HIF-1α target genes *LDHA* and *BNIP3* was observed in the PM2.5-treated cells, while calcitriol treatment resulted in decreased expression of *LDHA, BNIP3,* and *PDK1* genes (Fig. 6D-F). These findings suggest that calcitriol can suppress PM2.5-induced HIF-1α nuclear translocation and its downstream gene expression in BEAS-2B cells. Furthermore, calcitriol was observed to directly inhibit HIF-1α, as treatment with calcitriol alone substantially reduced the mRNA expressions of HIF-1α (Fig. 6A) and its target genes (Fig. 6D-F) compared to the sham-control group.

4. Discussion

PM2.5 can penetrate deeply into the lung and lead to lung injury via oxidative stress, inflammation and mitochondria dysfunction in human bronchial epithelial cells (Dominici et al., 2015; Toro-Heredia et al., 2021). Understanding the mechanisms underlying the adverse effects of PM2.5 on bronchial epithelial cells could provide insights into developing therapeutic and preventive strategies for air pollution-induced lung injury. Previous studies have suggested a beneficial role for the calcitriol/VDR axis in mitigating lung damage caused by the environmental insults including smoking and air pollution through antioxidant and anti-inflammatory properties (Liu et al., 2020; Slominski et al., 2020). In addition, PM2.5 exposure contributes to oxidative stress and inflammation possibly through mitochondrial damage in lung epithelial cells (Mori et al., 2021; Needs et al., 2021). Furthermore, HIF-1α, a key transcription factor in the oxygen-sensing system, plays a crucial role in mediating adaptive responses to oxidative insults by regulating various stress response mechanisms including mitochondrial bioenergetics (Liao and Zhang, 2020; Shi et al., 2021; Zuo and Wijegunawardana, 2021). This study aimed to investigate the protective role of the active vitamin D/VDR axis in PM2.5-induced oxidative stress and HIF-1α translocation involved in mitochondrial dysfunction in human bronchial epithelial cells.

Oxygen is a crucial for maintaining metabolic homeostasis and energy production necessary for cellular function. The oxidative phosphorylation system (OXPHOS) is the primary biochemical process for the electron transport chain within mitochondria. Exposure to environmental toxicants, including PM2.5, can stimulate the formation of ROS, leading to mitochondrial damage and exacerbating oxidative stress in a vicious cycle. Several studies have demonstrated that calcitriol specifically activates VDR and the calcitriol/VDR system can regulate various signaling cascades involved in antioxidant defense, inflammatory response and cellular metabolism (Colotta et al., 2017; Jeon and Shin, 2018). However, little is known about the involvement of the calcitriol/VDR axis in promoting mitochondrial function, particularly in relation to the regulation of HIF-1α nuclear translocation in lung epithelial cells. Our results revealed that calcitriol is capable of promoting the nuclear translocation of VDR (Fig. 3) and that the calcitriol/VDR system plays a protective role in PM2.5-mediated human lung epithelial BEAS-2B cell damage via suppression of intracellular ROS formation (Fig. 1) and restoration of mitochondrial bioenergetics (Fig. 2). VDR has previously been shown to play anti-apoptotic and anti-oxidative roles possibly via regulating mitochondrial function and the nuclear transcription of proteins involved in respiratory activity and ATP synthesis in MCF7 human breast cancer cells, HaCaT keratinocyte cell lines, and primary human fibroblasts (Ricca et al., 2018).

In response to ROS formation induced by environmental insults, HIF-1α is stabilized, driving the cells to adaptively respond to oxidative stress-induced injury in various tissues including the lungs (Liao and Zhang, 2020; Shi et al., 2021; Zuo and Wijegunawardana, 2021). Targeting HIF-1α offers potential therapeutic and preventive strategies for addressing disruptions in oxygen homeostasis associated with pathological conditions, including lung injury. In this study, PM2.5 exposure was shown to induce HIF-1α nuclear translocation and the expression of its target genes, including *LDHA*, *BNIP3*, and *PDK1*. This was associated with the downregulation of PGC-1α, the master regulator of mitochondrial biogenesis, and its downstream genes, including *SIRT3, CYCS, ATP5F1B* and *MnSOD* or *SOD2* (Fig. 4). Sirtuin-3 (Sirt3) functions as a mitochondrial tumor suppressor protein encoded by the *SIRT3* gene, suggesting a correlation between *SIRT3* expression and mitochondrial tumorigenesis under hypoxic condition (Bell et al., 2011). Cytochrome C Somatic (*CYCS*) gene encodes a protein associates with the inner mitochondrial membrane, accepting electrons from cytochrome b and transferring them to the cytochrome oxidase complex for further metabolic process in biogenesis (Kuang et al., 2020). ATP synthesis, a key product generated by mitochondrial protein complexes, involves the

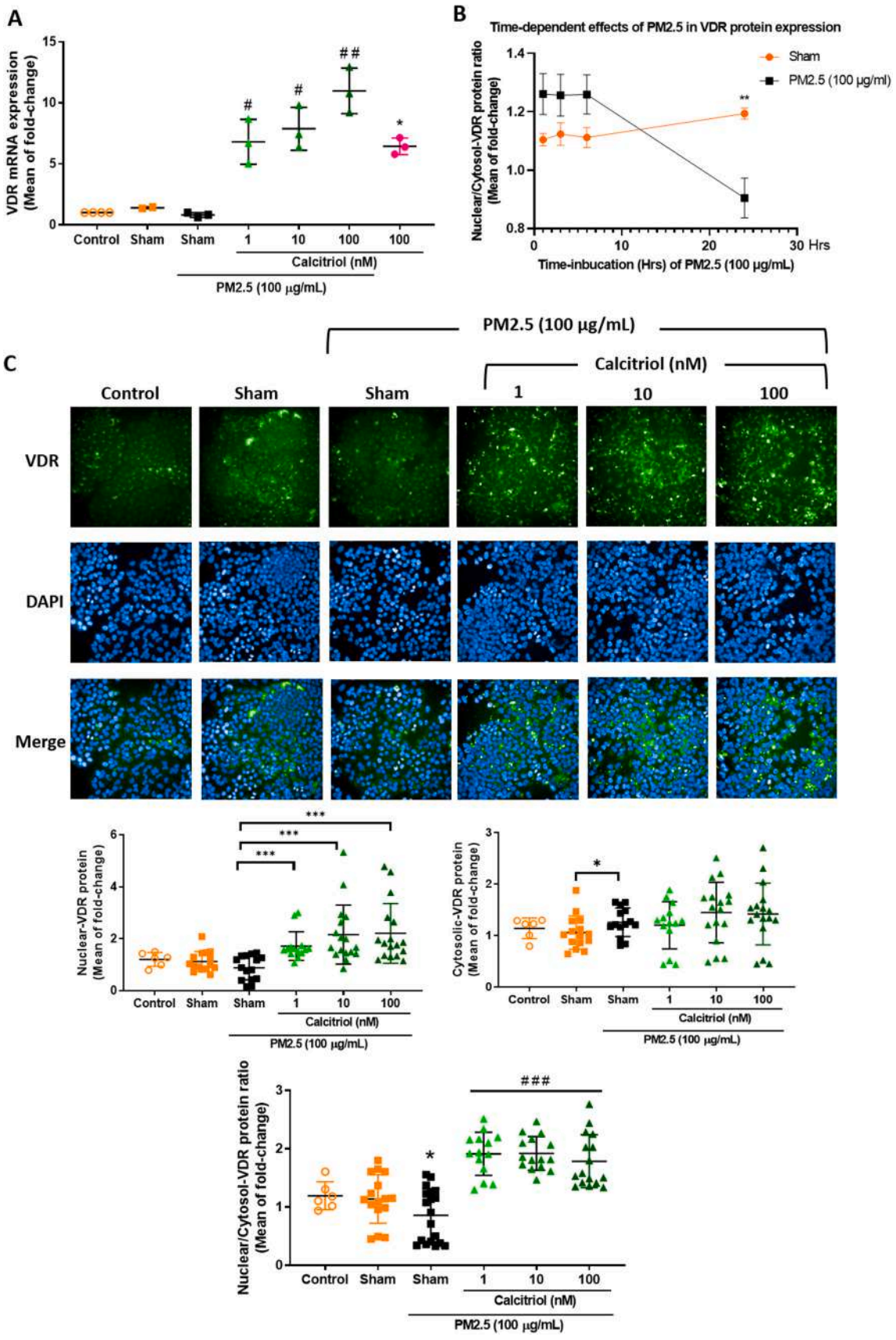

(caption on next page)

Fig. 5. The effects of PM2.5 and calcitriol, a vitamin D receptor (VDR) inducer, on VDR activation and VDR mRNA expression. (A) Real-time RT-PCR analysis of *VDR* mRNA expression. BEAS-2B cells treated with ethanol vehicle solution (1:1000 dilution; sham group) or 1, 10, 100 nM of calcitriol for 16 h prior to incubation with 100 μg/mL PM2.5 for 24 h. The mRNA levels (mean fold-change) were normalized relative to the GAPDH mRNA levels. (B) Time-dependent effects of PM2.5 on VDR nuclear translocation at 1, 3, 6, and 24 h. The dot plot graph represents the analysis of immunofluorescent imaging (nuclear/cytosolic protein ratio) using the Operetta CLS High-Content Analysis System (PerkinElmer Inc., USA). (C) Immunofluorescent imaging of treated cells incubated with each solution for 16 h prior to incubation with 100 μg/mL PM2.5 for 24 h. VDR protein was stained using anti-VDR conjugated to Alexa Fluor 488 and nuclei were counterstained with DAPI dye. The nuclear to cytosol ratio of VDR protein was evaluated as in the merged image. The dot plot graph shows the analysis of immunofluorescent imaging data. Data are presented as the nuclear/cytosolic VDR protein ratio (mean fold-change) and analyzed for statistical significance of differences using Student's *t* test (sham-control cells (orange dot) versus PM2.5-treated cells (black dot); $^{*}P<0.05$, $^{**}P< 0.01$; n $\geq$ 3), and one-way ANOVA with Dunnett's multiple comparison test (PM2.5-pretreated cells with calcitriol treatment (green dot) versus cells pretreated with PM2.5 alone (black dot).; $^{\#}P<0.05$, $^{\#\#}P< 0.01$, $^{\#\#\#}P< 0.001$; n $\geq$ 3).

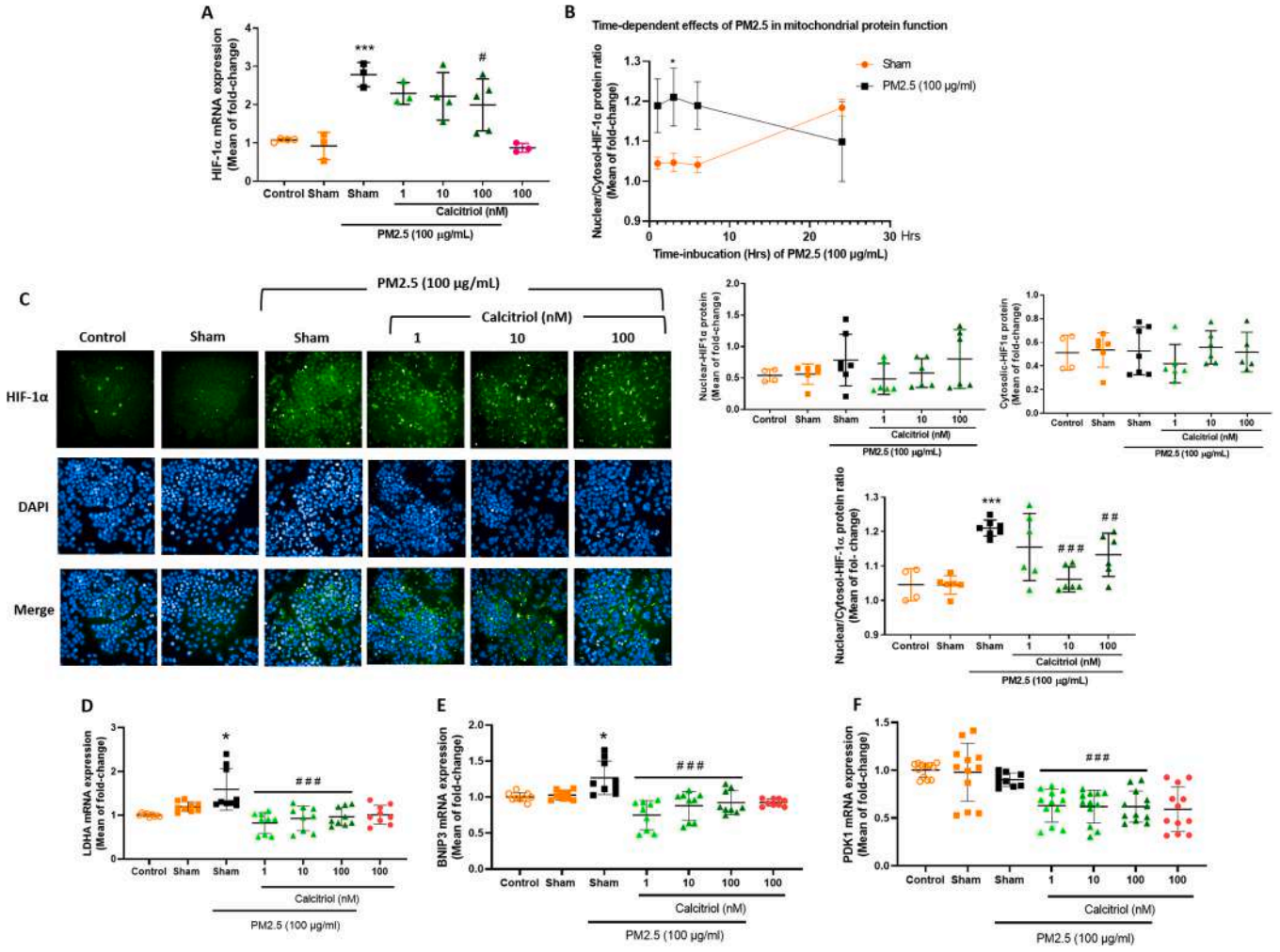

Fig. 6. Calcitriol ameliorated hypoxia-inducible factor-1α (HIF-1α) activation and its targeted genes expression in the PM2.5-treated cells. (A) Real-time RT-PCR analysis of *HIF-1α* mRNA expression. BEAS-2B cells treated with ethanol vehicle solution (1:1000 dilution; sham group) or 1, 10, 100 nM of calcitriol for 16 h prior to incubating with 100 μg/mL PM2.5 for 24 h. The mRNA levels (mean fold-change) were normalized relative to GAPDH mRNA levels. (B) Time-dependent effects of PM2.5 on HIF-1α protein expression at 1, 3, 6, and 24 h. The dot plot graph represents the analysis of immunofluorescent imaging (nuclear/cytosolic protein ratio) using the Operetta CLS High-Content Analysis System (PerkinElmer Inc., USA). (C) Fluorescent microscopy of cells stained with HIF-1α antibody tagged with FITC dye (green fluorescence), DAPI stained nuclei (blue fluorescence), and merge (dual fluorescent channels). BEAS-2B cells were treated with ethanol vehicle solution (1:1000 dilution; sham group) or 1, 10, 100 nM of calcitriol for 16 h prior to incubating with100 μg/mL PM2.5 for 3 h. (D-F) Real-time RT-PCR analysis of HIF-1α targeted genes: (D) *LDHA,* (E) *BNIP3,* and (F) *PDK1*. BEAS-2B cells were treated with ethanol vehicle solution (1:1000 dilution; sham group) or 1, 10, 100 nM of calcitriol for 16 h prior to incubating with100 μg/mL PM2.5 for 12 h. Data are presented as the nuclear/cytosolic HIF-1α protein ratio (mean fold-change) and analyzed for statistical significance of differences using Student's *t* test (sham-control cells (orange dot) versus PM2.5-treated cells (black dot); $^{**}P<0.01$, $^{***}P< 0.001$; n $\geq$ 3), and one-way ANOVA with Dunnett's multiple comparison test (PM2.5-pretreated cells with calcitriol treatment (green dot) versus cells pretreated with PM2.5 alone (black dot).; $^{\#}P<0.05$, $^{\#\#}P< 0.01$, $^{\#\#\#}P< 0.001$; n $\geq$ 3).

rotation of ATP synthase to balance the proton gradient in the mitochondrial matrix through OXPHOS reactions. ATP synthase F1 subunit beta (*ATP5F1B*) encodes a subunit of mitochondrial ATP synthase (Lu et al., 2018). Manganese superoxide dismutase (MnSOD) is an antioxidant enzyme present in mitochondria that protects against the mitochondrial oxidative damage (Li and Zhou, 2011). The nuclear translocation of HIFs (including HIF-1α) has been suggested to affect mitochondrial redox balance, biogenesis and functions including mitochondrial oxidative capacity, apoptosis and mitophagy (Bao et al., 2021; Huang et al., 2022; Slot et al., 2014). Our study suggests that

PM2.5-induced HIF-1α nuclear translocation might decrease mitochondrial biogenesis by targeting the transcriptional coactivator PGC-1α, a master controller of mitochondrial biogenesis and function in BEAS-2B cells. HIF-1α activation in response to PM2.5-induced oxidative stress could be involved in the interplay between calcitriol/VDR axis and mitochondrial signaling, which controls cell metabolism. It is important to note that HIF-1α can behave as either protective or harmful during inflammation or oxidative stress. Therefore, the double-edged sword role of HIF-1α in cellular homeostasis and its mechanism controlling mitochondrial biogenesis require further clarification.

5. Conclusion

In conclusion, targeting calcitriol/VDR system may serve as a promising pharmacological strategy for mitigating PM2.5-induced lung epithelial damage by promoting mitochondrial bioenergetics in association with the regulation of PGC-1α and HIF-1α signaling. As the primary metabolic hub, mitochondria play a crucial role in generating essential cellular metabolites and ROS. Changes in mitochondrial ROS and physiology will be further explored to elucidate the regulatory role of mitochondrial bioenergetics in PM2.5-mediated lung injury. Additionally, to support our *in vitro* evidence for the pharmacological potential of calcitriol, further studies using *in vivo* models of lung injury are warranted to develop calcitriol as an effective cytoprotective agent against air pollutants.

CRediT authorship contribution statement

Uraiwan Panich: Writing – review & editing, Writing – original draft, Supervision, Resources, Funding acquisition, Conceptualization. **Mutita Pluempreecha:** Validation, Methodology, Investigation. **Tanyapohn Soingam:** Validation, Methodology, Investigation. **Phetthinee Muanjumpon:** Validation, Methodology, Investigation. **Tasanee Onkoksong:** Validation, Methodology, Investigation. **Assistant Professor Anyamanee Chatsirisupachai:** Writing – review & editing, Writing – original draft, Visualization, Methodology, Funding acquisition, Conceptualization. **Saowanee Jeayeng:** Data curation, Formal analysis, Investigation, Methodology, Software, Writing – review & editing.

Declaration of Competing Interest

The authors declare that they have no known competing financial interests or personal relationships that could have appeared to influence the work reported in this paper.

Data Availability

No data was used for the research described in the article.

Acknowledgements and Funding

This work was supported by Chulabhorn Royal Academy; Office of the Permanent Secretary, Ministry of Higher Education, Science, Research and Innovation, Research Grant for New Scholar (RGNS), [Grant No. RGNS 63–246]; and the Mahidol University [Fundamental Fund: fiscal year 2023 by National Science Research and Innovation Fund (NSRF)].

Appendix A. Supporting information

Supplementary data associated with this article can be found in the online version at doi:10.1016/j.etap.2024.104568.

References

Annamalai, C., Seth, R., Viswanathan, P., 2021. Ferrotoxicity and its amelioration by calcitriol in cultured renal cells. Anal. Cell Pathol. 2021, 6634429. https://doi.org/10.1155/2021/6634429.

Ashcroft, S.P., Bass, J.J., Kazi, A.A., Atherton, P.J., Philp, A., 2020. The vitamin D receptor regulates mitochondrial function in C2C12 myoblasts. Am. J. Physiol. Cell Physiol. 318, C536–C541. https://doi.org/10.1152/ajpcell.00568.2019.

Bao, X., Zhang, J., Huang, G., Yan, J., Xu, C., Dou, Z., Sun, C., Zhang, H., 2021. The crosstalk between HIFs and mitochondrial dysfunctions in cancer development. Cell Death Dis. 12, 215. https://doi.org/10.1038/s41419-021-03505-1.

Bell, E.L., Emerling, B.M., Ricoult, S.J., Guarente, L., 2011. SirT3 suppresses hypoxia inducible factor 1alpha and tumor growth by inhibiting mitochondrial ROS production. Oncogene 30, 2986–2996. https://doi.org/10.1038/onc.2011.37.

Bhattarai, H.K., Shrestha, S., Rokka, K., Shakya, R., 2020. Vitamin D, calcium, parathyroid hormone, and sex steroids in bone health and effects of aging. J. Osteoporos. 2020, 9324505. https://doi.org/10.1155/2020/9324505.

Bikle, D.D., 2014. Vitamin D metabolism, mechanism of action, and clinical applications. Chem. Biol. 21, 319–329. https://doi.org/10.1016/j.chembiol.2013.12.016.

Boland, M.L., Chourasia, A.H., Macleod, K.F., 2013. Mitochondrial dysfunction in cancer. Front. Oncol. 3, 292. https://doi.org/10.3389/fonc.2013.00292.

Calahorra, J., Martinez-Lara, E., De Dios, C., Siles, E., 2018. Hypoxia modulates the antioxidant effect of hydroxytyrosol in MCF-7 breast cancer cells. PLoS One 13, e0203892. https://doi.org/10.1371/journal.pone.0203892.

Cao, Q., Rui, G., Liang, Y., 2018. Study on PM2.5 pollution and the mortality due to lung cancer in China based on geographic weighted regression model. BMC Public Health 18, 925. https://doi.org/10.1186/s12889-018-5844-4.

Chaiprasongsuk, A., Janjetovic, Z., Kim, T.K., Schwartz, C.J., Tuckey, R.C., Tang, E.K.Y., Raman, C., Panich, U., Slominski, A.T., 2020. Hydroxylumisterols, photoproducts of pre-Vitamin D3, protect human keratinocytes against UVB-induced damage. Int. J. Mol. Sci. 21. https://doi.org/10.3390/ijms21249374.

Chaiprasongsuk, A., Lohakul, J., Soontrapa, K., Sampattavanich, S., Akarasereenont, P., Panich, U., 2017. Activation of Nrf2 reduces UVA-mediated MMP-1 upregulation via MAPK/AP-1 signaling cascades: the photoprotective effects of sulforaphane and Hispidulin. J. Pharm. Exp. Ther. 360, 388–398. https://doi.org/10.1124/jpet.116.238048.

Chakraborti, S., Parinandi, N., Ghosh, R., Ganguly, N., Chakraborti, T., 2020. Oxid. Stress Lung Dis. https://doi.org/10.1007/978-981-32-9366-3.

Colotta, F., Jansson, B., Bonelli, F., 2017. Modulation of inflammatory and immune responses by vitamin D. J. Autoimmun. 85, 78–97. https://doi.org/10.1016/j.jaut.2017.07.007.

Dai, J., Sun, C., Yao, Z., Chen, W., Yu, L., Long, M., 2016. Exposure to concentrated ambient fine particulate matter disrupts vascular endothelial cell barrier function via the IL-6/HIF-1alpha signaling pathway. FEBS Open Bio 6, 720–728. https://doi.org/10.1002/2211-5463.12077.

Ding, H., Jiang, M., Li, D., Zhao, Y., Yu, D., Zhang, R., Chen, W., Pi, J., Chen, R., Cui, L., Zheng, Y., Piao, J., 2021. Effects of real-ambient PM2.5 exposure on lung damage modulated by Nrf2(-/). Front. Pharmacol. 12, 662664. https://doi.org/10.3389/fphar.2021.662664.

Dominguez, L.J., Farruggia, M., Veronese, N., Barbagallo, M., 2021. Vitamin D sources, metabolism, and deficiency: available compounds and guidelines for its treatment. Metabolites 11. https://doi.org/10.3390/metabo11040255.

Dominici, F., Wang, Y., Correia, A.W., Ezzati, M., Pope, C.A., 3rd, Dockery, D.W., 2015. Chemical composition of fine particulate matter and life expectancy: in 95 US counties between 2002 and 2007. Epidemiology 26, 556–564. https://doi.org/10.1097/EDE.0000000000000297.

Gaspar, J.M., Velloso, L.A., 2018. Hypoxia inducible factor as a central regulator of metabolism - implications for the development of obesity. Front. Neurosci. 12, 813. https://doi.org/10.3389/fnins.2018.00813.

Gesmundo, I., Silvagno, F., Banfi, D., Monica, V., Fanciulli, A., Gamba, G., Congiusta, N., Libener, R., Riganti, C., Ghigo, E., Granata, R., 2020. Calcitriol inhibits viability and proliferation in human malignant pleural mesothelioma cells. Front. Endocrinol. 11, 559586. https://doi.org/10.3389/fendo.2020.559586.

Gonzalez, S.M., Aguilar-Jimenez, W., Trujillo-Gil, E., Zapata, W., Su, R.C., Ball, T.B., Rugeles, M.T., 2019. Vitamin D treatment of peripheral blood mononuclear cells modulated immune activation and reduced susceptibility to HIV-1 infection of CD4+ T lymphocytes. PLoS One 14, e0222878. https://doi.org/10.1371/journal.pone.0222878.

Guo, H., Li, W., Wu, J., 2020. Ambient PM2.5 and annual lung cancer incidence: a nationwide study in 295 Chinese counties. Int. J. Environ. Res. Public Health 17. https://doi.org/10.3390/ijerph17051481.

Huang, K., Li, W., Chen, Y., Zhu, J., 2018. Effect of PM2.5 on invasion and proliferation of HeLa cells and the expression of inflammatory cytokines IL-1 and IL-6. Oncol. Lett. 16 (6), 7068–7073. https://doi.org/10.3892/ol.2018.9516.

Huang, X., Zhao, L., Peng, R., 2022. Hypoxia-inducible factor 1 and mitochondria: an intimate connection. Biomolecules 13. https://doi.org/10.3390/biom13010050.

Jeon, S.M., Shin, E.A., 2018. Exploring vitamin D metabolism and function in cancer. Exp. Mol. Med. 50, 1–14. https://doi.org/10.1038/s12276-018-0038-9.

Jiang, P., Hao, S., Xie, L., Xiang, G., Hu, W., Wu, Q., Liu, Z., Li, S., 2021. LncRNA NEAT1 contributes to the acquisition of a tumor like-phenotype induced by PM 2.5 in lung bronchial epithelial cells via HIF-1alpha activation. Environ. Sci. Pollut. Res. Int. 28, 43382–43393. https://doi.org/10.1007/s11356-021-13735-7.

Jin, X., Su, R., Li, R., Cheng, L., Li, Z., 2018. Crucial role of pro-inflammatory cytokines from respiratory tract upon PM2.5 exposure in causing the BMSCs differentiation in cells and animals. Oncotarget 9, 1745–1759. https://doi.org/10.18632/oncotarget.23158.

Kierans, S.J., Taylor, C.T., 2021. Regulation of glycolysis by the hypoxia-inducible factor (HIF): implications for cellular physiology. J. Physiol. 599, 23–37. https://doi.org/10.1113/JP280572.

Kim, K.H., Kabir, E., Kabir, S., 2015. A review on the human health impact of airborne particulate matter. Environ. Int. 74, 136–143. https://doi.org/10.1016/j.envint.2014.10.005.

Kim, H.A., Perrelli, A., Ragni, A., Retta, F., De Silva, T.M., Sobey, C.G., Retta, S.F., 2020. Vitamin D deficiency and the risk of cerebrovascular disease. Antioxidants 9. https://doi.org/10.3390/antiox9040327.

Kuang, F., Liu, J., Tang, D., Kang, R., 2020. Oxidative damage and antioxidant defense in ferroptosis. Front. Cell Dev. Biol. 8, 586578. https://doi.org/10.3389/fcell.2020.586578.

Lelieveld, S., Wilson, J., Dovrou, E., Mishra, A., Lakey, P.S.J., Shiraiwa, M., Poschl, U., Berkemeier, T., 2021. Hydroxyl radical production by air pollutants in epithelial lining fluid governed by interconversion and scavenging of reactive oxygen species. Environ. Sci. Technol. 55, 14069–14079. https://doi.org/10.1021/acs.est.1c03875.

Li, R., Wang, Y., Qiu, X., Xu, F., Chen, R., Gu, W., Zhang, L., Yang, S., Cai, Z., Liu, C., 2020. Difference on oxidative stress in lung epithelial cells and macrophages induced by ambient fine particulate matter (PM2.5). Air Qual. Atmos. Health 13, 789–796. https://doi.org/10.1007/s11869-020-00835-5.

Li, C., Zhou, H.M., 2011. The role of manganese superoxide dismutase in inflammation defense. Enzym. Res. 2011, 387176. https://doi.org/10.4061/2011/387176.

Li, H.S., Zhou, Y.N., Li, L., Li, S.F., Long, D., Chen, X.L., Zhang, J.B., Feng, L., Li, Y.P., 2019. HIF-1alpha protects against oxidative stress by directly targeting mitochondria. Redox Biol. 25, 101109. https://doi.org/10.1016/j.redox.2019.101109.

Liao, C., Zhang, Q., 2020. Understanding the oxygen-sensing pathway and its therapeutic implications in diseases. Am. J. Pathol. 190, 1584–1595. https://doi.org/10.1016/j.ajpath.2020.04.003.

Lin, J., Puigserver, P., Donovan, J., Tarr, P., Spiegelman, B.M., 2002. Peroxisome proliferator-activated receptor gamma coactivator 1beta (PGC-1beta), a novel PGC-1-related transcription coactivator associated with host cell factor. J. Biol. Chem. 277, 1645–1648. https://doi.org/10.1074/jbc.C100631200.

Liu, H.L., Chuang, H.Y., Hsu, C.N., Lee, S.S., Yang, C.C., Liu, K.T., 2020. Effects of Vitamin D Receptor, Metallothionein 1A, and 2A Gene Polymorphisms on Toxicity of the Peripheral Nervous System in Chronically Lead-Exposed Workers. Int. J. Environ. Res Public Health 17. https://doi.org/10.3390/ijerph17082909.

Liu, C.-W., Lee, T.-L., Chen, Y.-C., Liang, C.-J., Wang, S.-H., Lue, J.-H., Tsai, J.-S., Lee, S.-W., Chen, S.-H., Yang, Y.-F., Chuang, T.-Y., Chen, Y.-L., 2018. PM2.5-induced oxidative stress increases intercellular adhesion molecule-1 expression in lung epithelial cells through the IL-6/AKT/STAT3/NF-κB-dependent pathway. Part. Fibre Toxicol. 15, 4. https://doi.org/10.1186/s12989-018-0240-x.

Lohakul, J., Jeayeng, S., Chaiprasongsuk, A., Torregrossa, R., Wood, M.E., Saelim, M., Thangboonjit, W., Whiteman, M., Panich, U., 2022. Mitochondria-targeted hydrogen sulfide delivery molecules protect against UVA-induced photoaging in human dermal fibroblasts, and in mouse skin in vivo. Antioxid. Redox Signal 36, 1268–1288. https://doi.org/10.1089/ars.2020.8255.

Lu, Y., Ma, J., Song, Z., Ye, Y., Fu, P.P., Lin, G., 2018. The role of formation of pyrrole-ATP synthase subunit beta adduct in pyrrolizidine alkaloid-induced hepatotoxicity. Arch. Toxicol. 92, 3403–3414. https://doi.org/10.1007/s00204-018-2309-6.

Luo, Y., Ma, J., Lu, W., 2020. The significance of mitochondrial dysfunction in cancer. Int. J. Mol. Sci. 21. https://doi.org/10.3390/ijms21165598.

Mazuryk, O., Stochel, G., Brindell, M., 2020. Variations in reactive oxygen species generation by urban airborne particulate matter in lung epithelial cells-impact of inorganic fraction. Front. Chem. 8, 581752. https://doi.org/10.3389/fchem.2020.581752.

McGarry, T., Biniecka, M., Veale, D.J., Fearon, U., 2018. Hypoxia, oxidative stress and inflammation. Free Radic. Biol. Med. 125, 15–24. https://doi.org/10.1016/j.freeradbiomed.2018.03.042.

Mori, M.P., Penjweini, R., Knutson, J.R., Wang, P.Y., Hwang, P.M., 2021. Mitochondria and oxygen homeostasis. FEBS J. https://doi.org/10.1111/febs.16115.

Needs, H.I., Protasoni, M., Henley, J.M., Prudent, J., Collinson, I., Pereira, G.C., 2021. Interplay between mitochondrial protein import and respiratory complexes assembly in neuronal health and degeneration. Life 11. https://doi.org/10.3390/life11050432.

Niu, B.Y., Li, W.K., Li, J.S., Hong, Q.H., Khodahemmati, S., Gao, J.F., Zhou, Z.X., 2020. Effects of DNA damage and oxidative stress in human bronchial epithelial cells exposed to PM(2.5) from Beijing, China, in winter. Int. J. Environ. Res Public Health 17. https://doi.org/10.3390/ijerph17134874.

O'Hagan, K.A., Cocchiglia, S., Zhdanov, A.V., Tambuwala, M.M., Cummins, E.P., Monfared, M., Agbor, T.A., Garvey, J.F., Papkovsky, D.B., Taylor, C.T., Allan, B.B., 2009. PGC-1alpha is coupled to HIF-1alpha-dependent gene expression by increasing mitochondrial oxygen consumption in skeletal muscle cells. Proc. Natl. Acad. Sci. USA 106, 2188–2193. https://doi.org/10.1073/pnas.0808801106.

Olszewska, A.M., Sieradzan, A.K., Bednarczyk, P., Szewczyk, A., Zmijewski, M.A., 2022. Mitochondrial potassium channels: a novel calcitriol target. Cell Mol. Biol. Lett. 27, 3. https://doi.org/10.1186/s11658-021-00299-0.

Orakij, W., Chetiyanukornkul, T., Chuesaard, T., Kaganoi, Y., Uozaki, W., Homma, C., Boongla, Y., Tang, N., Hayakawa, K., Toriba, A., 2017. Personal inhalation exposure to polycyclic aromatic hydrocarbons and their nitro-derivatives in rural residents in northern Thailand. Environ. Monit. Assess. 189, 510. https://doi.org/10.1007/s10661-017-6220-z.

Pinichka, C., Makka, N., Sukkumnoed, D., Chariyalertsak, S., Inchai, P., Bundhamcharoen, K., 2017. Burden of disease attributed to ambient air pollution in Thailand: a GIS-based approach. PLoS One 12, e0189909. https://doi.org/10.1371/journal.pone.0189909.

Pun, V.C., Kazemiparkouhi, F., Manjourides, J., Suh, H.H., 2017. Long-term PM2.5 exposure and respiratory, cancer, and cardiovascular mortality in older US adults. Am. J. Epidemiol. 186, 961–969. https://doi.org/10.1093/aje/kwx166.

Quesada-Gomez, J.M., Entrenas-Castillo, M., Bouillon, R., 2020. Vitamin D receptor stimulation to reduce acute respiratory distress syndrome (ARDS) in patients with coronavirus SARS-CoV-2 infections: revised Ms SBMB 2020_166. J. Steroid Biochem. Mol. Biol. 202, 105719. https://doi.org/10.1016/j.jsbmb.2020.105719.

Ricca, C., Aillon, A., Bergandi, L., Alotto, D., Castagnoli, C., Silvagno, F., 2018. Vitamin D receptor is necessary for mitochondrial function and cell health. Int. J. Mol. Sci. 19. https://doi.org/10.3390/ijms19061672.

Shan, H., Li, X., Ouyang, C., Ke, H., Yu, X., Tan, J., Chen, J., Wang, C., Zhang, L., Tang, Y., Yu, L., Li, W., 2022. Salidroside prevents PM2.5-induced BEAS-2B cell apoptosis via SIRT1-dependent regulation of ROS and mitochondrial function. Ecotoxicol. Environ. Saf. 231, 113170. https://doi.org/10.1016/j.ecoenv.2022.113170.

Shi, J., Yu, T., Song, K., Du, S., He, S., Hu, X., Li, X., Li, H., Dong, S., Zhang, Y., Xie, Z., Li, C., Yu, J., 2021. Dexmedetomidine ameliorates endotoxin-induced acute lung injury in vivo and in vitro by preserving mitochondrial dynamic equilibrium through the HIF-1a/HO-1 signaling pathway. Redox Biol. 41, 101954. https://doi.org/10.1016/j.redox.2021.101954.

Slominski, A.T., Chaiprasongsuk, A., Janjetovic, Z., Kim, T.K., Stefan, J., Slominski, R.M., Hanumanthu, V.S., Raman, C., Qayyum, S., Song, Y., Song, Y., Panich, U., Crossman, D.K., Athar, M., Holick, M.F., Jetten, A.M., Zmijewski, M.A., Zmijewski, J., Tuckey, R.C., 2020. Photoprotective properties of Vitamin D and lumisterol hydroxyderivatives. Cell Biochem. Biophys. 78, 165–180. https://doi.org/10.1007/s12013-020-00913-6.

Slot, I.G., Schols, A.M., Vosse, B.A., Kelders, M.C., Gosker, H.R., 2014. Hypoxia differentially regulates muscle oxidative fiber type and metabolism in a HIF-1alpha-dependent manner. Cell Signal 26, 1837–1845. https://doi.org/10.1016/j.cellsig.2014.04.016.

Stenton, S.L., Prokisch, H., 2020. Genetics of mitochondrial diseases: identifying mutations to help diagnosis. EBioMedicine 56, 102784. https://doi.org/10.1016/j.ebiom.2020.102784.

Tan, Z.X., Chen, Y.H., Xu, S., Qin, H.Y., Wang, H., Zhang, C., Xu, D.X., Zhao, H., 2016. Calcitriol inhibits tumor necrosis factor alpha and macrophage inflammatory protein-2 during lipopolysaccharide-induced acute lung injury in mice. Steroids 112, 81–87. https://doi.org/10.1016/j.steroids.2016.05.005.

Tanakol, R., Gul, N., Uzum, A.K., Aral, F., 2018. Calcitriol treatment in patients with low vitamin D levels. Arch. Osteoporos. 13, 114. https://doi.org/10.1007/s11657-018-0529-2.

Toro-Heredia, J., Jirau-Colón, H., Jiménez-Vélez, B.D., 2021. Linking PM2.5 organic constituents, relative toxicity and health effects in Puerto Rico. Environ. Chall. 5, 100350. https://doi.org/10.1016/j.envc.2021.100350.

Tretli, S., Schwartz, G.G., Torjesen, P.A., Robsahm, T.E., 2012. Serum levels of 25-hydroxyvitamin D and survival in Norwegian patients with cancer of breast, colon, lung, and lymphoma: a population-based study. Cancer Causes Control 23, 363–370. https://doi.org/10.1007/s10552-011-9885-6.

Veerappan, I., Sankareswaran, S.K., Palanisamy, R., 2019. Morin protects human respiratory cells from PM2.5 induced genotoxicity by mitigating ROS and reverting altered miRNA expression. Int. J. Environ. Res. Public Health 16. https://doi.org/10.3390/ijerph16132389.

Wiwanitkit, V., 2016. Thai waste landfill site fire crisis, particular matter 10, and risk of lung cancer. J. Cancer Res. Ther. 12, 1088–1089. https://doi.org/10.4103/0973-1482.172120.

Wu, J., Shi, Y., Asweto, C.O., Feng, L., Yang, X., Zhang, Y., Hu, H., Duan, J., Sun, Z., 2017. Fine particle matters induce DNA damage and G2/M cell cycle arrest in human bronchial epithelial BEAS-2B cells. Environ. Sci. Pollut. Res. Int. 24, 25071–25081. https://doi.org/10.1007/s11356-017-0090-3.

Yang, X., Zhao, T., Feng, L., Shi, Y., Jiang, J., Liang, S., Sun, B., Xu, Q., Duan, J., Sun, Z., 2019. PM2.5-induced ADRB2 hypermethylation contributed to cardiac dysfunction through cardiomyocytes apoptosis via PI3K/Akt pathway. Environ. Int. 127, 601–614. https://doi.org/10.1016/j.envint.2019.03.057.

Yeh, C.L., Wu, J.M., Chen, K.Y., Wu, M.H., Yang, P.J., Lee, P.C., Chen, P.D., Yeh, S.L., Lin, M.T., 2022. Effects of different routes and forms of vitamin D administration on CD4(+) T cell homeostasis and renin-angiotensin system-associated lung injury in obese mice complicated with polymicrobial sepsis. Biomed. Pharmacother. 156, 113961. https://doi.org/10.1016/j.biopha.2022.113961.

Yeh, C.L., Wu, J.M., Su, L.H., Yang, P.J., Lee, P.C., Chen, K.Y., Yeh, S.L., Lin, M.T., 2021. Intravenous calcitriol administration regulates the renin-angiotensin system and attenuates acute lung injury in obese mice complicated with polymicrobial sepsis. Biomed. Pharmacother. 141, 111856. https://doi.org/10.1016/j.biopha.2021.111856.

Zhang, X., Harbeck, N., Jeschke, U., Doisneau-Sixou, S., 2017. Influence of vitamin D signaling on hormone receptor status and HER2 expression in breast cancer. J. Cancer Res. Clin. Oncol. 143, 1107–1122. https://doi.org/10.1007/s00432-016-2325-y.

Zuo, L., Wijegunawardana, D., 2021. Redox role of ROS and inflammation in pulmonary diseases. Adv. Exp. Med Biol. 187–204. https://doi.org/10.1007/978-3-030-68748-9_11.